Journal of Coastal Research	17	3	544–552	West Palm Beach, Florida	Summer 2001

The Influence of River Discharge on Salinity Intrusion in the Tanshui Estuary, Taiwan

Wen-Cheng Liu,† Ming-Hsi Hsu,‡ Albert Y. Kuo,¶ and Jan-Tai Kuo*

†Hydrotech Research Institute
National Taiwan University
Taipei 10617, Taiwan

‡Department of Agricultural Engineering and Hydrotech Research Institute
National Taiwan University
Taipei 10617, Taiwan

¶School of Marine Science
Virginia Institute of Marine Science
The College of William and Mary
Gloucester Point, VA 23062, U.S.A.

*Department of Civil Engineering and Hydrotech Research Institute
National Taiwan University
Taipei 10617, Taiwan

ABSTRACT

LIU, W-C.; HSU, M-H.; KUO, A.Y., and KUO, J-T., 2001. The influence of river discharge on salinity intrusion in the Tanshui Estuary, Taiwan. *Journal of Coastal Research,* 17(3), 544–552. West Palm Beach (Florida), ISSN 0749-0208.

The Tanshui River system is the largest estuarine system in Taiwan, with drainage basin including the capital city of Taipei. It consists of three major tributaries: the Tahan Stream, Hsintien Stream and Keelung River. A vertical two-dimensional numerical model is refined and expanded to handle tributaries as well as the main stem of an estuarine system, and applied to the Tanshui River estuarine system.

Observed time series of salinity data and tidal-averaged salinity distributions have been compared with model results to calibrate the turbulent diffusion coefficients. The overall model verification is suggested to be achieved with comparisons of residual currents and salinity distribution. The agreement between observed data and computed results put the stamp of approval on the model. The model is shown capable of reproducing the prototype water surface elevation, currents and salinity distributions. This paper emphasizes model applications. As an example of model utilities, the calibrated and verified model is used to calculate the salinity distributions under various conditions. The salinity distributions are simulated and compared under several scenarios of wastewater diversion and under various hydrological conditions to examine their response to the amount of freshwater inflows in the Tanshui River system. We find that the Tanshui River system is a partially mixed estuary in most instances and its salinity is very sensitive to river discharge. The model is also used to investigate the salinity response to the pulse of high freshwater discharge. The salinity has a very quick response and recovers to its original condition in about 7 days. The calculated estuary flushing time was strongly dependent on river flow and varied between hours to a month.

ADDITIONAL INDEX WORDS: *Estuary, salinity intrusion, numerical model, freshwater discharge, model application, Tanshui estuary, Taiwan.*

INTRODUCTION

To predict hydraulic transport of materials in streams to an estuary and then into the ocean one requires understanding of river discharge rates and water movement in estuary. The hydrodynamic characteristics of tidal rivers have properties of fluvial (unidirectional) flow and marine nearshore (bi-directional) flow. The former includes seasonal and transient variations of freshwater discharge while the latter is dominated by tide, and complicated by salt-freshwater interaction as well as meteorological events.

Numerical models designed to simulate transport process in estuaries should provide a detailed account of both advective and turbulent diffusive transport of materials. Many vertical-longitudinal hydrodynamic models ($x - z$ models) have been developed and used in estuarine studies (JOHNSON, 1981). The type of model may be either purely vertical-longitudinal (assumes rectangular cross section), or just laterally averaged. HAMILTON (1975) developed a vertical two-dimensional numerical model of rectangular geometry to study circulation in the Rotterdam Waterway, *i.e.,* nonlinear governing equations were derived in Cartesian coordinates and simplified by assuming that all channel cross sections were rectangular. BLUMBERG (1975; 1977; 1978), ELLIOTT (1976) and RAO (1995) included nonuniform geometry in their two-dimensional models of the Chesapeake Bay, Potomac River, and Godavari estuary. BOERICKE and HOGAN (1977) developed a laterally averaged model to study the effects of thermal discharge on the dynamics of the lower Hudson River. WANG and KRAVITZ (1980) developed a semi-implicit, two-dimensional model for circulation of a partially mixed estuary. Application of their model to the Potomac River indicated large longitudinal and vertical changes in tidal, density-driven and wind-driven circulation, which suggested that two-dimensional (in a vertical plane) modeling is essential in the transport and mixing study. Their results, together with observations indicated that the advection and mixing processes in a narrow, partially mixed estuary can be properly modeled by including the vertical dimension. EDINGER and BUCHAK (1981) modified a computer application originally developed to study laterally averaged reservoir circulation and applied it to the Potomac River estuary. The nonlinear equations in conservative form were solved in Cartesian coordinates by

00012 received 5 February 2000; accepted in revision 17 July 2000.

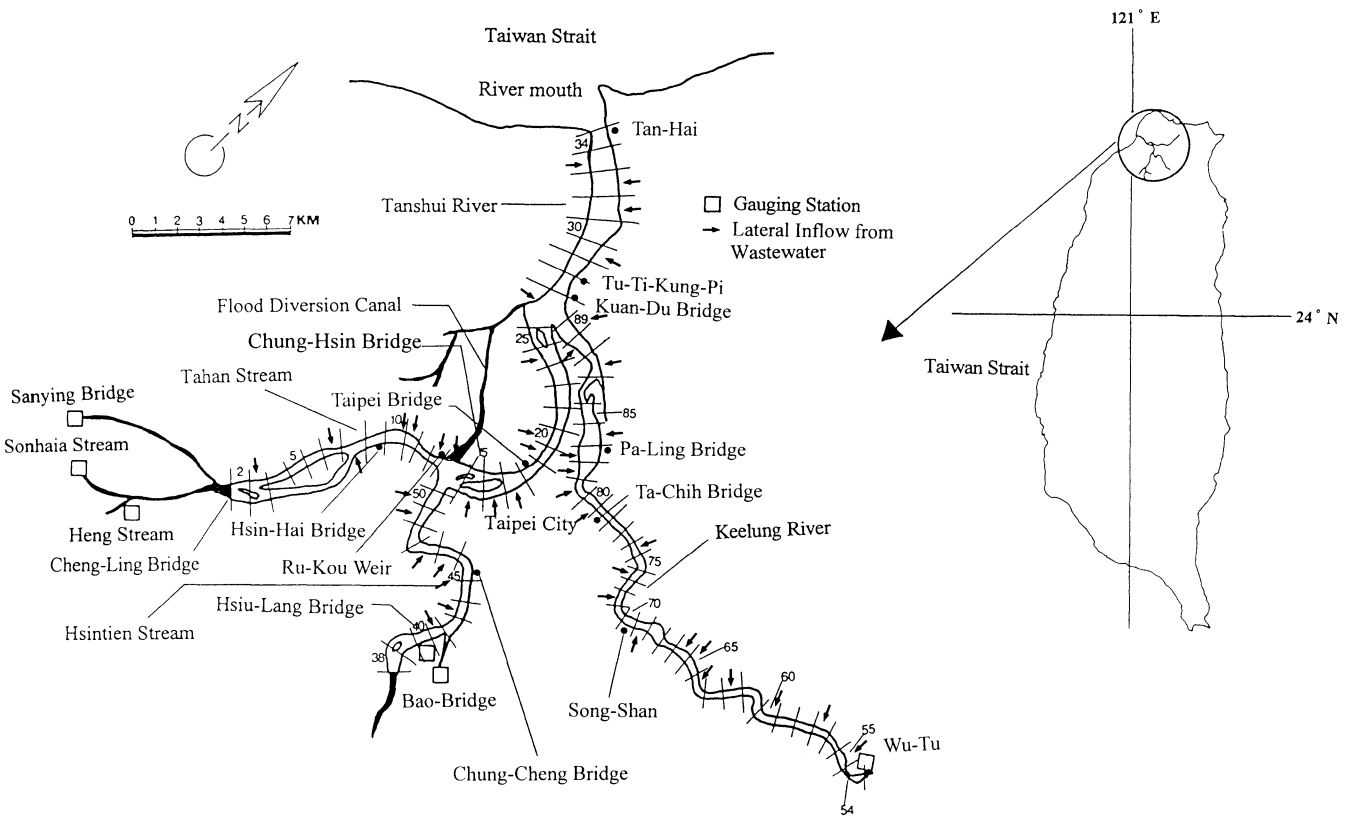

Figure 1. Map of the Tanshui River System and the model segments.

finite difference methods. PERRELS and KARELSE (1981) developed a laterally averaged model with branching network capabilities to study circulation in the Rotterdam Waterway.

Objectives of the present study are to gain additional insight into the vertical variations of hydrodynamic properties in the Tanshui estuary and to determine how these properties are affected by fluvial freshwater discharge variations and by oceanic tides. Since vertical variations are present mainly in the deep channels of the estuary, a suitable laterally averaged model may reproduce primary estuarine processes occurring in the deep channels.

Numerical models can quantify such processes over a wider range of river flow conditions than might be possible with a field program. In addition, a properly calibrated model provides information on salinity distribution throughout the full length of the estuary, rather than at necessarily limited and selective sampling locations. In this study, a laterally integrated, two-dimensional, real-time model of hydrodynamics and salinity is developed and expanded to handle tributaries as well as the main stem of an estuarine system, and applied to the Tanshui River estuary.

STUDY AREA

The Tanshui River is formed by the confluence of Tahan Stream, Hsintein Stream and Keelung River (Figure 1). Downstream portions of all three tributaries are influenced by tide, and subjected to sea water intrusion. Together, they form the largest estuarine system in Taiwan. The major portion of the estuarine system, upstream of Kuan-Du (Figure 1), lies within the Taipei basin, while the stretch downstream is confined by high mountains on both sides. In addition, the river is narrow that there is no significant wind-induced current in the river. The major forcing mechanisms of the flows are astronomical tide at river mouth and river discharges at upriver ends. Semi-diurnal tides are the principal tidal constituents, with a mean tidal range of 2.22 m and a spring tidal range of 3.1 m. The average river discharges at the upstream limits of tide are 62.1 m^3/s, 72.7 m^3/s, 26.1 m^3/s, respectively, in the Tahan Stream, Hsintien Stream and Keelung River. The river system has a total drainage area of 2726 km^2, and a total channel length of 327.6 km. The average slope of the study reach is about 0.022 on 100. In addition to the barotropic flows forced by river discharges and tides, the baroclinic flow caused by density difference is another important transport mechanism in the Tanshui River estuary system.

Six million people, over a quarter of Taiwan entire population, reside in the catchment area of the Tanshui River system. The river system receives untreated domestic discharge and both treated and untreated industrial effluents; thus, it is heavily polluted. The upper estuary is normally suboxic and gradually becomes oxic in the lower estuary with increasing dilution by sea water (CHEN and HUNG, 1988).

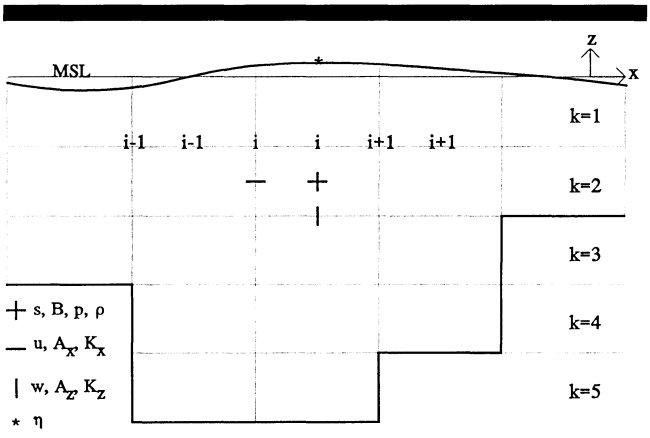

Figure 2. Grid pattern, location and indexing of variables.

The dynamic processes involving the interaction between river discharge and tidal currents are complex and lead to a series of distinctive types of estuarine circulation in the Tanshui estuary. A numerical model was used to simulate the complex circulation patterns. Observed time series salinity and tidally-averaged salinity distributions are compared with model results to validate the turbulent diffusive coefficients. The model was shown capable of reproducing the observed circulation and salinity conditions (HSU *et al.,* 1999). A brief description of model calibration and verification procedures are presented in the next section. This paper emphasizes model applications. The salinity distributions are simulated and compared under several scenarios of wastewater diversion and various hydrological conditions. The model is also used to investigate the salinity response to the pulse of high freshwater discharge. The flushing time of the estuary is also calculated.

DESCRIPTION AND CALIBRATION OF THE MODEL

The laterally integrated two-dimensional hydrodynamic model developed by KUO *et al.* (1978) was modified for application to the Tanshui River system. The original version is applicable only to a single stem estuary. The model is expanded to include the simulation of tributaries which is necessary because of the three major tributaries in the tidal portion of the system. Assumptions for the validity of the governing equations are: (1) variations of dependent variables in the transverse direction are small and negligible and (2) the lateral average of the transverse velocity component is zero. The hydrostatic approximation and the Boussinesq approximation are also assumed to be valid (BLUMBERG, 1977). With a right-handed Cartesian coordinate system with the x-axis directed seaward and the z-axis directed upward (Figure 2), the governing equations may be written as followings. The continuity equations are

$$\frac{\partial(uB)}{\partial x} + \frac{\partial(wB)}{\partial z} = q_p \tag{1}$$

where u and w = laterally averaged velocities in the x- and z- directions, respectively, B = river width, q_p = lateral inflow per unit bank area, and

$$\frac{\partial}{\partial t}(B_\eta \eta) + \frac{\partial}{\partial x}\int_H^\eta (uB)\, dz = q \tag{2}$$

where t = time, η = position of the free surface above mean sea level, B_η = river width at the free surface including side storage area, H = total depth below mean sea level, q = lateral inflow per unit river length. Equations (1) and (2) are the laterally and sectionally, respectively, integrated continuity equations for incompressible flow. The momentum balance equation is

$$\frac{\partial(uB)}{\partial t} + \frac{\partial(uBu)}{\partial x} + \frac{\partial(uBw)}{\partial z} = -\frac{B}{\rho}\frac{\partial p}{\partial x} + \frac{\partial}{\partial x}\left(A_x B\frac{\partial u}{\partial x}\right) + \frac{\partial}{\partial z}\left(A_z B\frac{\partial u}{\partial z}\right) \tag{3}$$

where p and ρ = pressure and density, respectively, A_x and A_z = turbulent viscosities in the x- and z- directions, respectively. This is the laterally integrated equation of motion for incompressible, but non-homogeneous flow and represents the momentum balance along the longitudinal axis of an estuary. The hydrostatic equation is

$$\frac{\partial p}{\partial z} = -\rho g \tag{4}$$

where g = gravitational acceleration. When the hydrostatic approximation (i.e., gravity is the dominant force in the vertical direction) is applied to the equation of motion in the z-direction, the result is the hydrostatic solution given by equation (4). The laterally integrated mass balance equation for dissolved salt is

$$\frac{\partial(sB)}{\partial t} + \frac{\partial(sBu)}{\partial x} + \frac{\partial(sBw)}{\partial z} = \frac{\partial}{\partial x}\left(K_x B\frac{\partial s}{\partial x}\right) + \frac{\partial}{\partial z}\left(K_z B\frac{\partial s}{\partial z}\right) + S_o \tag{5}$$

where s = laterally averaged salinity, K_x and K_z = turbulent diffusivities in the x- and z- directions, respectively, S_o = source and sink of salt water. The equation of state is

$$\rho = \rho_o(1 + ks) \tag{6}$$

where ρ_o = density of fresh water and a constant $k = 7.5 \times 10^{-4}$ ppt^{-1}. The density is related to the salinity by the simplified equation of state (equation (6)), which is usually regarded as a satisfactory approximation because of the large spatial gradients of salinity in estuaries (HAMILTON 1977). The turbulent closure model uses the Munk-Anderson type formulations:

$$A_z = \alpha Z^2\left(1 - \frac{Z}{h}\right)^2\left|\frac{\partial u}{\partial z}\right|(1 + \beta R_i)^{-1/2} + \alpha_w\frac{H_w^2}{T}\exp\left(-\frac{2\pi}{L}Z\right) \tag{7}$$

$$K_z = \alpha Z^2\left(1 - \frac{Z}{h}\right)^2\left|\frac{\partial u}{\partial z}\right|(1 + \beta R_i)^{-3/2} + \alpha_w\frac{H_w^2}{T}\exp\left(-\frac{2\pi}{L}Z\right) \tag{8}$$

where Z and h = distance from the surface and total depth ($h = \eta + H$), R_i = local Richard number, H_w, T and L =

height, period and length, respectively, of wind-induced waves, α, β and α_w = constants.

The system of equations is solved using finite difference method with uniform grid of spatially staggered variables. Equations (1) to (3) are solved to obtain the time-varying solution of the free surface (η) and laterally averaged velocity fields (u and w). The pressure term (p) is evaluated using equation (4) with the water density (ρ) from equation (6), and salinity (s) using equation (5). The detailed description of the method of solution including boundary conditions, turbulence closure model, treatment of the interaction of tributaries and main stem, and stability criteria can be found in HSU *et al.* (1996; 1997).

The layout of the grid system used in the model and locations of variables within the grid are shown in Figure 2. The grid system has η defined at the middle of each segment, while s, B, ρ and p at the center of the grid cell. The variables, w, A_z and K_z, are defined at the bottom face of the grid cell, while the grid containing u, A_x and K_x is staggered by half the segment length as these are defined at the grid cell walls. The staggered grid structure, also used by many other investigators, permits easy application of the boundary conditions and evaluation of the dominant pressure gradient force without interpolation or averaging (BLUMBERG, 1977).

In the application to the Tanshui estuarine system, the model treats the Tanshui River and Tahan Stream as the main stem and Hsintien Stream and Keelung River as tributaries. They are divided into 33, 14, and 37 segments, respectively, with a uniform segment length of 1.0 km. The vertical grid spacing is 1 m for all layers, except the surface layer which is variable, with 2 m at mean sea level. Details of model calibration and verification have been presented in HSU *et al.* (1996; 1997; 1999). In the following, a brief description is presented.

Manning's friction coefficient and the coefficients for turbulent mixing terms are important calibration parameters affecting the calculation of surface elevation, current velocity and salinity distribution. The preliminary calibration of Manning's friction coefficient used a single constituent tide, M_2, to reproduce the longitudinal distribution of mean tidal range. The results show the average absolute values of differences (mean absolute errors) between computed and measured tidal ranges is 3.4 cm, while the root-mean-square error is 3.8 cm, both of which are less than 2% of mean tidal range. The fine-tune calibration compares the along-river variations of amplitude and phase of the individual constituent, using a nine-constituent tide to force the system at river mouth. The results also compare times of high tide and low tide between computation and observation. The difference in the model results and observations are less than 10 minutes. The calibrated model has the Manning's friction coefficient ranging from 0.032 to 0.026 in the Tanshui River-Tahan Stream, 0.015 for the Hsintien Stream, and from 0.023 to 0.016 for the Keelung River.

The calibration of mixing processes was conducted through model simulation of prototype conditions during the period March 15 to September 30, 1994. The model was driven by three time-varying boundary conditions: measured daily freshwater inflow through the upstream boundaries, hourly tidal elevation and linearly interpolated salinity from measured data at the river mouth. The upstream boundary conditions were specified with daily freshwater discharges at Cheng-Ling Bridge (Tahan Stream), Hsui-Lang Bridge (Hsintien Stream), and Wu-Tu station (Keelung River). The tidal average salinity and time series data measured on April 12 and June 24, 1994 were used to calibrate the constants in the formulation of vertical diffusion coefficient. The results show the mean absolute errors and root-mean-square errors of the difference between the computed and hourly measured data are from 0.13 to 1.76 ppt and from 0.16 to 2.45 ppt, respectively, at various stations.

The model's ability to predict mass transport was verified with a simulation of salinity distribution from March 15 to April 30, 1995. The model predictions agree well with the field measurements on April 14, 1995. The results show the mean absolute errors and root-mean-square errors of the difference between the computed and hourly measured data are from 0.12 to 1.44 ppt and from 0.13 to 1.62 ppt, respectively, at various stations.

MODEL APPLICATION AND DISCUSSION

The Influence of Discharge Variation

The validated model was used to perform a series of model simulations to investigate salinity distributions in the Tanshui River system under various hydrological conditions. The values of all coefficients of the numerical model have been determined by calibration and verification processes; no further adjustment to the coefficients was made.

The time series data of surface elevation at river mouth, collected by the Taiwan Water Conservancy Agency, were examined and harmonic analyses were performed. Residual surface elevation and energy ratio are used to judge the harmonic results. Residual surface elevation is the root-mean square of the difference between the synthetic tide and observed surface elevation and the energy ratio represents the ratio of energy of water surface fluctuation of synthetic tide to that of observed tide. HSU *et al.* (1999) concluded that nine constituent tides represent adequately the tidal conditions. Therefore, a nine-constituent tide was used to specify the downstream boundary condition for the following model experiments. For the harmonic analysis, the surface elevation η is presented in the form:

$$\eta(t) = \langle\eta\rangle + \sum_k a_k \cos(\sigma_k t - \phi_k) \quad (9)$$

where a_k and ϕ_k are the amplitude and phase angle of the kth harmonic, respectively; $\langle\eta\rangle$ is the mean surface elevation; σ_k is angular velocity. Table 1 lists the amplitudes and phases of the primary nine tidal constituents at the river mouth. Historical long-term mean (15-year average) water surface elevation is +6.5 cm relative to mean sea level. For the first model simulation, historical long-term mean (34-year average) discharges were used for the upriver boundary conditions in the tributaries. Mean discharges at the tidal upstream limits are 62.1 m^3/s, 72.7 m^3/s and 26.1 m^3/s for the Tahan Stream, Hsintien Stream and Keelung River, respectively. Salinity at the Tanshui River mouth was set at 25 ppt

Table 1. *The amplitudes and phases of the primary nine tidal constituents at the Tanshui River mouth.*

Constituents	Amplitude cm	Phase Degree
M_2	104.87	35.60
S_2	27.85	−7.18
N_2	21.33	−43.76
K_1	19.94	−133.79
S_a	17.06	−143.32
O_1	16.22	−47.96
K_2	7.17	131.50
P_1	7.14	−110.58
M_4	2.83	47.44

under mean flow condition. The model was run for one-year duration (705 tidal cycles). Figure 3 presents the predicted salinity distributions averaged over 2 spring-neap cycles (*i.e.,* 58 tidal cycles) in the Tanshui River-Tahan Stream, Keelung River and Hsintien Stream. The limit of salt intrusion is represented by the 1 ppt isohaline. Signification stratification occurs only in the first 10 km at the downstream end of the Tanshui River, since estuarine circulation occurs only in deep water at this reach of the river under mean flow conditions. The residual circulation tends to be strongest in deep section of the estuary and in the region where the salinity gradient is largest. The limits of salt intrusion are located at the Chung-Hsin Bridge in the Tahan Stream and 6 km from the Keelung River mouth. There is barely any salt intrusion in the Hsintien Stream.

Another model simulation was conducted using the Q_{75} flow condition (Q_{75} is the annually flow that is equaled or exceeded 75% of time). Q_{75} discharges at the tidal upstream limits of the three major tributaries are 8.15 m^3/s, 20.2 m^3/s and 3.61 m^3/s for Tahan Stream, Hsintien Stream, and Keelung River, respectively. The 25 ppt salinity at the Tanshui River mouth was used for boundary condition, the same as the mean flow simulation in order to investigate the effects of different freshwater discharges. The model was run for one-year (705 tidal cycles). Figure 4 presents the average salinity distribution over 2 spring-neap cycles (*i.e.,* 58 tidal cycles) in the Tanshui River-Tahan Stream, Keelung River, and Hsintien Stream. The limits of salt intrusion are located at the Hsin-Hai Bridge in the Tahan Stream, 11 km from the Keelung River mouth, and 4 km from the Hsintein Stream mouth. The extensive intrusion of saline water introduces a significant baroclinic forcing and induces a strong residual circulatory system in the estuary.

Comparing figures 3 and 4, it is clear that higher river flow (mean flow) pushes the limits of salt intrusion farther downriver than low flow (Q_{75}) condition. With a weakening of the river flow, tidal action becomes more dominant and induces more mixing of salt and freshwater over the water column. However, the increased baroclinic circulation not only force the more saline bottom water upriver but also increases vertical stratification. The balance between tidal mixing and baroclinic circulation ultimately determines vertical salinity structures, which vary from location to location. River discharge is a dominant factor in determining salinity distribution.

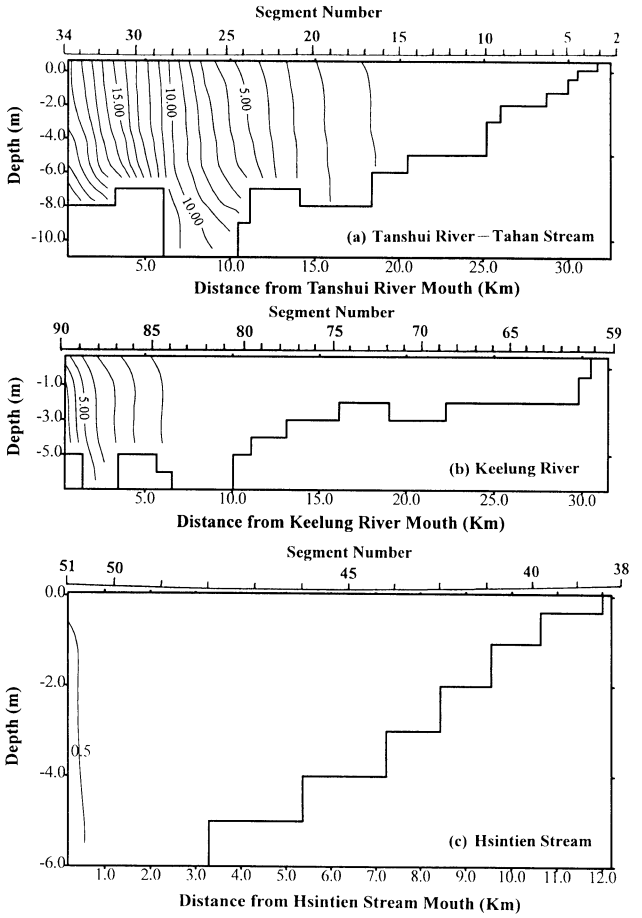

Figure 3. Calculated salinity distributions averaged over 58 tidal cycles under mean flow conditions (a) Tanshui River-Tahan Stream (b) Keelung River (c) Hsintien Stream. (Numbers on the contours refer to the salinity in parts per thousand)

Figure 5 presents the time series surface elevation and salinity under mean and Q_{75} flow conditions. Salinity shows a strong periodic fluctuation in response to tide, with high stratification at low tide and nearly well-mixed at high tide. Baroclinic circulation enhances the vertical velocity shear, increasing stratification by differential advection during ebb tide. Both the reduced differential advection and enhanced mixing during flood help to eliminate stratification. Net downstream advection counters upstream progression of salt water along the bottom of the estuary, and partially mixed conditions are attained.

Reduction of Freshwater Input

The model was also run with Q_{75} flows at upstream boundaries while the lateral inflow from wastewater along the river (shown in Figure 1) was cut-off by sewage interception systems which is being constructed. The diversion of a large amount of wastewater to the ocean outfall system will decrease the freshwater flow in the river. A detailed analysis of salinity distributions was made for two cases,

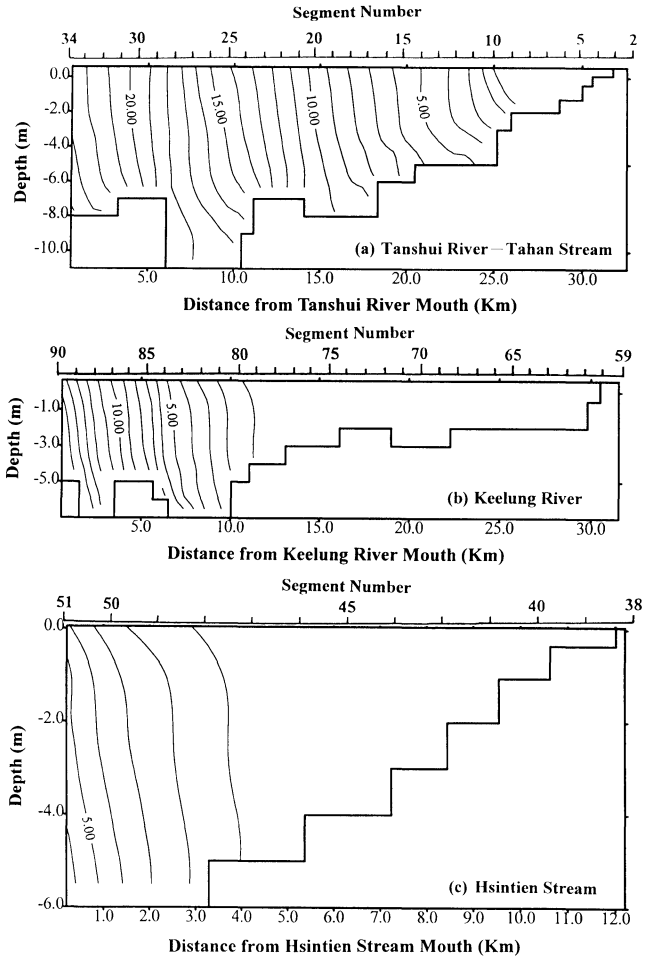

Figure 4. Calculated salinity distributions averaged over 58 tidal cycles under Q_{75} flow conditions (a) Tanshui River-Tahan Stream (b) Keelung River (c) Hsintien Stream. (Numbers on the contours refer to the salinity in parts per thousand)

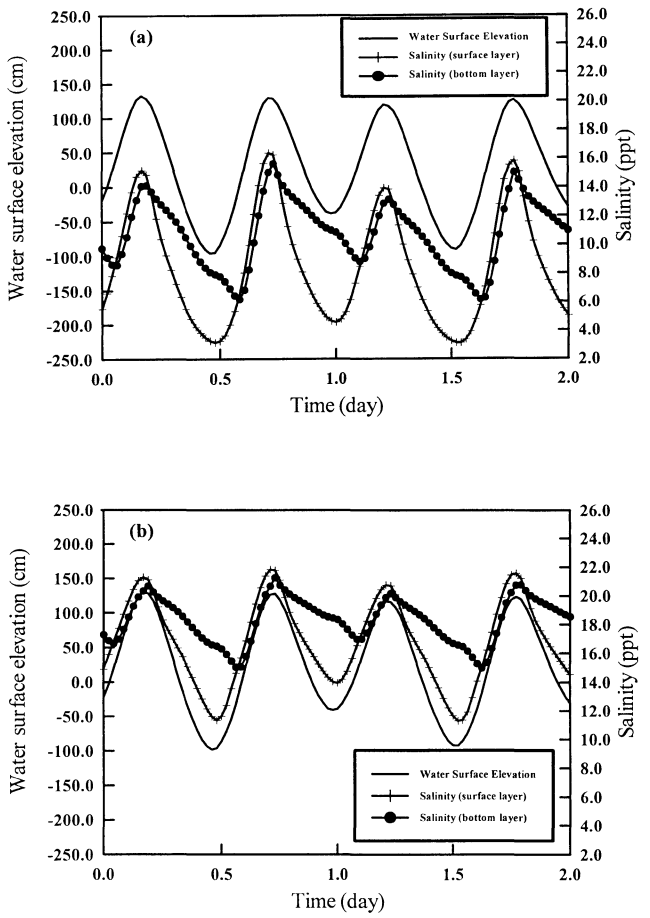

Figure 5. Time series surface elevation and salinity at Kuan-Du Bridge (a) mean flow condition (b) Q_{75} flow condition.

60% and 100% wastewater diversion, respectively. Table 2 shows freshwater discharge imposed at upstream boundary conditions and the lateral inflow from watershed below gauging stations and from wastewater. Figures 6 and 7 present the tidally-averaged salinity distributions under the two cases. Comparing with the simulation results without wastewater diversion (shown in Figure 4), figures 6 and 7 show that salinity increases about 1~2 ppt in most part of the estuary as a result of wastewater diversion. However, the limits of salt intrusion move only slightly upriver even if the wastewater is totally cut-off. Inspection of the bathymetric profile indicates that the limits of salt intrusion stay near the sills (*i.e.,* where the river bottom rises rapidly in the upriver direction). The sills at the upriver ends play an important role to prevent further salt intrusion as freshwater input diminishes.

Transient Response to High Freshwater Discharge

The Q_{50} measure was used as the base condition to investigate the salinity response to a pulse of high freshwater discharge. The model was run with Q_{50} to attain an equilibrium state condition before a high freshwater pulse of two days duration was introduced. The Q_{50} flow at the tidal limits of the three major tributaries are 17.6 m^3/s, 44.5 m^3/s and 9.8 m^3/s for the Tahan Stream, Hsintien Stream and Keelung River, respectively. Salinity at the Tanshui River mouth was set at 30 ppt. A simple sinusoidal (M_2) tide with an amplitude equal to the mean at the Tanshui River mouth (111.2 cm) was used to force the hydrodynamic model. High freshwater discharge was imposed on the upstream boundaries of the

Table 2. *Freshwater discharges imposed at upstream boundary conditions and lateral inflow.*

Upstream Freshwater Discharge/Lateral Inflow	Q_{75} Flow Condition cm^3/s
Tahan Stream	8.15
Hsintien Stream	20.2
Keelung River	3.61
Lateral inflow from watershed	7.6
Lateral inflow from wastewater	20.63
Cut-off 60% wastewater	8.25
Cut-off 100% wastewater	0

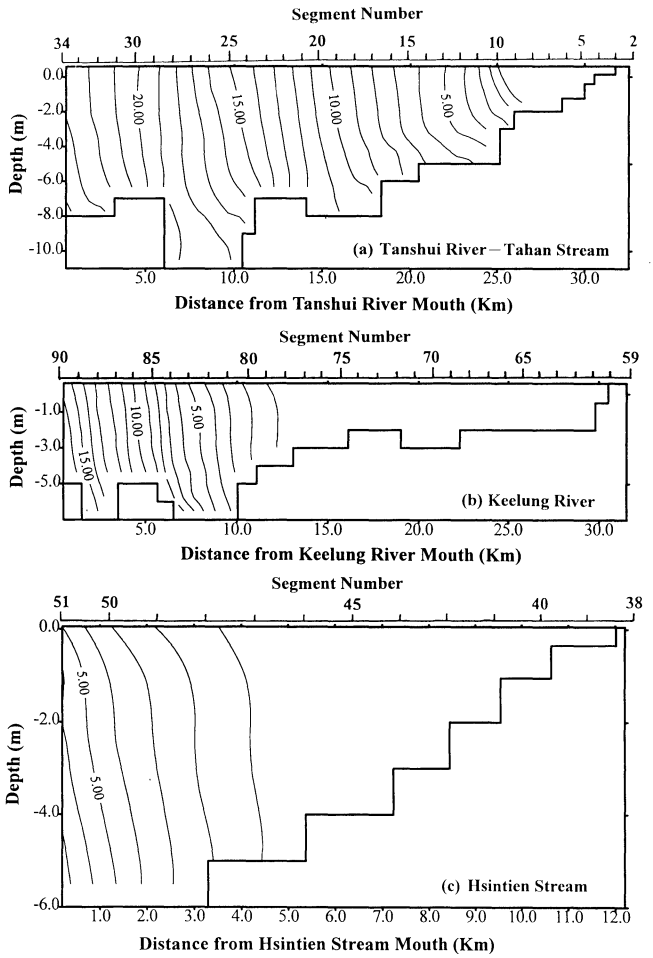

Figure 6. Calculated salinity distributions averaged over 58 tidal cycles with 60 percentage wastewater cut-off (a) Tanshui River-Tahan Stream (b) Keelung River (c) Hsintien Stream. (Numbers on the contours refer to the salinity in parts per thousand)

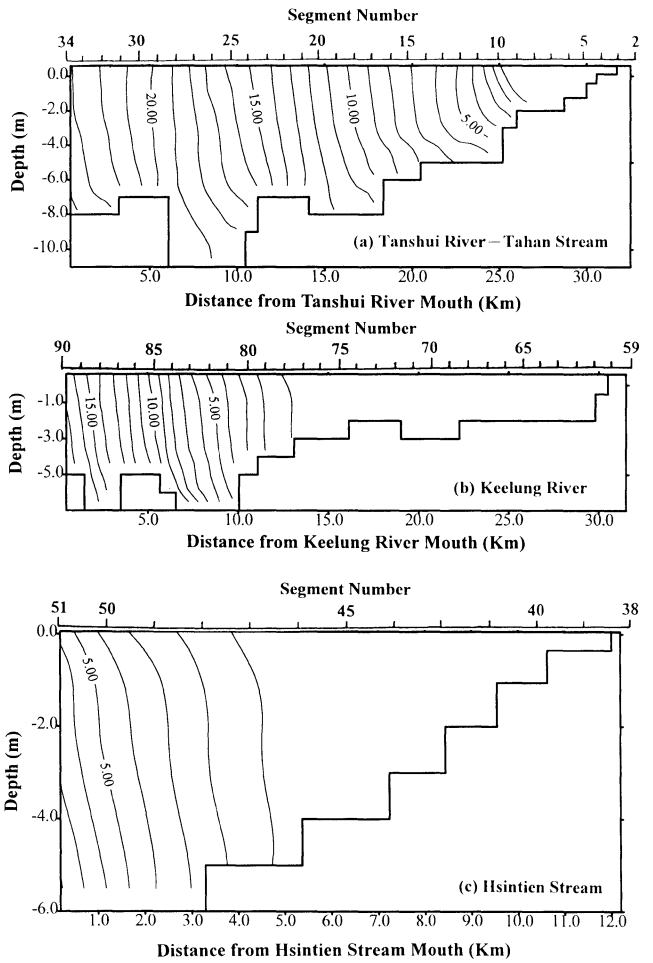

Figure 7. Calculated salinity distributions averaged over 58 tidal cycles with total wastewater cut-off (a) Tanshui River-Tahan Stream (b) Keelung River (c) Hsintien Stream. (Numbers on the contours refer to the salinity in parts per thousand)

three major tributaries for two calendar days. Figure 8 presents the time series salinity responses to the pulse of high freshwater discharge. Aftermath of high flow, salinity gradually recovers to its original condition in about 5, 9, and 7 days in the Tahan Stream, Hsintien Stream and Keelung River, respectively. These recovering times are quite different from the larger estuarine system, (*e.g.,* the major tributary estuaries of the Chesapeake Bay, USA) which require an order of a month to recover to normal conditions (NICHOLS, 1993).

Flushing Time

The estuarine flushing time was also estimated from a series of model simulations. The flushing time is defined as the time taken to replace the existing fresh water in the estuary at a rate equal to the river discharge (DYER, 1973; OFFICER, 1976), *i.e.,* $T_f = F/R$ where F is the total volume of fresh water in the estuary at high water and R is the river discharge. The model simulations were performed for a range of river discharge conditions. In this study, it is the flushing time of the entire tidal portion of the Tanshui River system we were investigating, not just the portion of the river conforming to the strict definition of estuary (*i.e.* saline portion of the river). Therefore the total volume of freshwater in the entire model domain was calculated from model results of salinity distribution and river geometry. Figure 9 presents the estimated flushing time as a function of river discharge. The increase in river discharge is accompanied by a more rapid exchange of freshwater with the sea. The volume of fresh water accumulated in the estuary increases with a lesser extent than does the discharge. Thus the flushing time decreases with increasing river discharge.

Figure 9 shows that the flushing time varies between 36 to 1077 hours over the range of river discharge investigated, and is inversely related to river discharge. For river discharges above 12.2 m^3/s, the flushing time is less than 1077 hours. For the very low river discharges, the flushing time increases

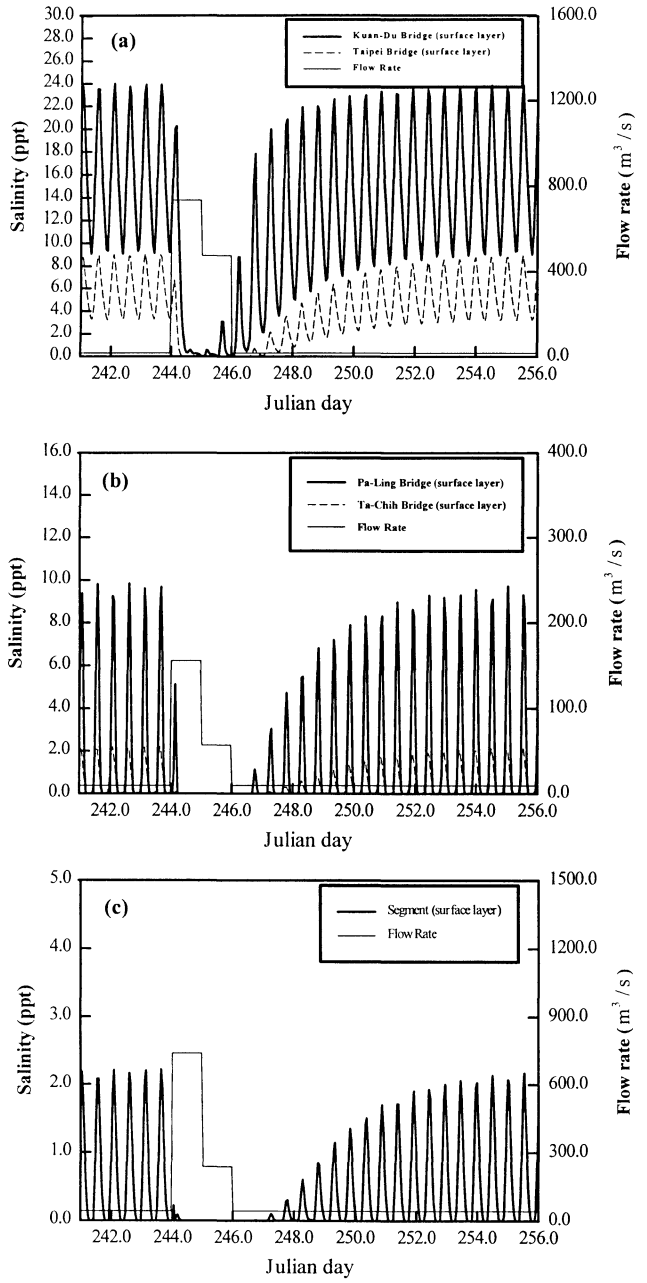

Figure 8. Time series salinity response to the pulse of high freshwater discharge.

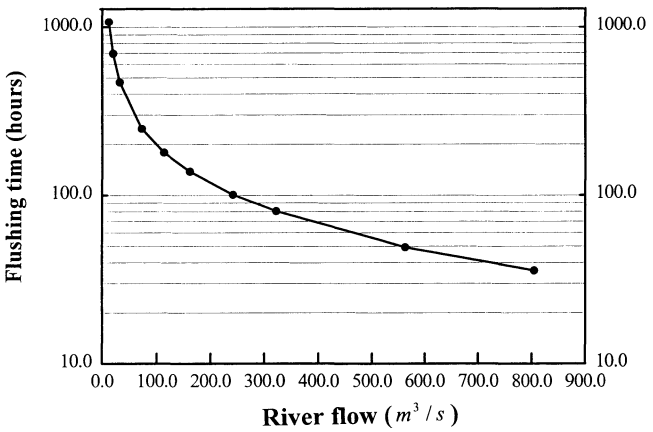

Figure 9. Estimates of the flushing time of the estuary calculated for a range of river discharges.

sharply but changes slowly at high river discharge, which is similar to the estimates given by KETCHUM (1952).

CONCLUSIONS

A numerical model has been developed to study the hydrodynamic characteristics and salinity distributions of a branched estuary in northern Taiwan. The model is a laterally integrated, two-dimensional, real-time model. The model was applied to the Tanshui River estuary, and calibrated and verified with observed time series water level, current, and salinity data and spatial distributions of tidally-averaged salinity. Analyses were made of the computed salinity distributions under several scenarios of wastewater diversion and under various hydrological conditions to investigate their responses to the amount of freshwater inflows in the Tanshui River estuarine system.

The magnitude of river discharge is the dominant factor affecting salinity intrusion in the estuary. Under mean flow conditions, sea water barely intrudes into the Hsintein Stream. Reduction of the river discharge to Q_{75} flow increases the extent of salt intrusion by 7 km, 5 km and 4 km in the Tahan Stream, Keelung River and Hsintein Stream, respectively.

Simulation of flow reduction with lateral inflow cut-off by sewage interception systems shows salinity increase over the entire estuary. The level of increase is 1 to 2 ppt under the Q_{75} modeled condition. Salinity increase is expected to be more severe under lower flow conditions. Limits of salt intrusion shift only slightly upriver in all branches of the river. Under low flow conditions, limits of salt intrusion are primarily control by river bathymetry at upriver ends.

The model was also used to investigate the salinity response to the pulse of high freshwater discharge. Salinity recovers quickly to normal conditions in less than 5, 9, and 7 days for the Tanshui River-Tahan Stream, Hsintien Stream and Keelung River, respectively. The calculated system flushing time is strongly dependent on river flow and varies between hours to an order of one month.

ACKNOWLEDGEMENTS

The project under which this study was conducted was supported, in part, by National Science Council, R.O.C., under grant No. 88-2611-E-002-036 and 89-2213-E-002-075. The financial support in highly appreciated. The authors also like to express their appreciation to the two manuscript reviewers; though their comments and suggestions this paper was substantially improved.

LITERATURE CITED

BLUMBERG, A. F., 1975. A numerical investigation into the dynamics of estuarine circulation. Chesapeake Bay Institute, Technical Report 91, The Johns Hopkins University, 59p.

BLUMBERG, A. F., 1977. Numerical tidal model of Chesapeake Bay. *Journal of the Hydraulic Division,* ASCE, 103, 295–319.

BLUMBERG, A. F., 1978. The influence of density variations on estuarine tides and circulation. *Estuarine and Coastal Marine Science,* 6, 209–215.

BOERICKE, R. R. and HOGAN, J. M., 1977. An x-z hydraulic/thermal model for estuarine. *Journal of the Hydraulic Division, Proceedings ASCE,* 103(HY1), 19–37.

CHEN, Y. C. and HUNG, T. C., 1988. The behavior and mobilization of trace metals in the Tanshui River. *Journal of the Environmental Protection Society of the Republic of china,* 11, 21–31. (in Chinese)

DYER, K. R., 1973. *Estuaries: A Physical Introduction.* New York: Wiley, 140p.

EDINGER, J. E. and BUCHAK, E. M., 1981. Estuarine laterally averaged numerical dynamics: the development and testing of estuarine boundary conditions in the LARM code. Paper EL-81-9, Prepared by J. E. Edinger Associates Inc., for the U.S. Army Engineering Waterways Experiment Station, CE, Vicksburg, Mississippi, 84p.

ELLIOTT, A. J., 1976. A numerical model of the internal circulation in a branching estuary. Chesapeake Bay Institute, Special Report 54, The Johns Hopkins University, 85p.

HAMILTON, P., 1975. A numerical model of the vertical circulation of tidal estuaries and its application to the Rotterdam Waterway. *Journal of Geophysical Research, Astronomy Society,* 40, 1–21.

HAMILTON, P., 1977. On the numerical formation of a time dependent multi-level model of an estuary, with particular reference to boundary conditions. *In:* WILEY, M. (Editor): *Estuarine Processes: Volume II Circulation, Sediment and Transfer of Material in the Estuary.* New York: Academic Press Inc, 347–364.

HSU, M. H.; KUO, A. Y.; KUO, J. T., and LIU, W. C., 1996, 1997. Study of tidal characteristics, estuarine circulation and salinity distribution in Tanshui River system (1), (2). Technical Report No. 239 and 273, Hydrotech Research Institute. National Taiwan University, Taipei, Taiwan, 245p. (in Chinese)

HSU, M. H.; KUO, A. Y.; KUO, J. T., and LIU, W. C., 1999. Procedure to calibrate and verify numerical models of estuarine hydrodynamics. *Journal of the Hydraulic Engineering, ASCE,* 125, 166–182.

JOHNSON, B. H., 1981. A review of numerical reservoir hydrodynamic modeling. Technical Report E-81-2, U.S. Army Waterways Experiment Station, Hydraulic Laboratory, Vicksburg, Mississippi, 41p.

KETCHUM, B. H., 1952. Circulation in estuaries. Proceedings 3rd Conference Coastal Engineering, 65–76.

KUO, A. Y.; NICHOLS, M., and LEWIS, J., 1978. Modeling sediment movement in the turbidity maximum of an estuary. Bulletin 111, Virginia Water Resources Research Center, Virginia Polytechnic Institute and State University, Blacksburg, Virginia, 76p.

NICHOLS, M., 1993. Response of coastal plain estuaries to episodic events in the Chesapeake Bay region. *In:* MEHTA, A. (Editor): *Nearshore and Estuarine Cohesive Sediment Transport.* New York: Springer-Verlag, 1–20.

OFFICER, C. B., 1976. *Physical Oceanography of Estuaries (and Associated Coastal Waters).* New York: Wiley, 465p.

PERRELS, P. A. J. and KARELSE, M., 1981. A two-dimensional laterally averaged model for salt intrusion in estuaries. *In:* FISHER, H. B. (Editor): *Transport Models for Inland and Coastal Waters.* San Diego: Academic Press, 483–535.

RAO, A. D., 1995. A numerical modelling study of the flow and salinity structures in the Godavari estuary, east coast of India. *International Journal for Numerical Methods in Fluids,* 21, 35–48.

WANG, D. P. and KRAVITZ, D. W., 1980. A semi-implicit two-dimensional model of estuarine circulation. *Journal of Physical Oceanography,* 10, 441–451.